Photophysics of Arylene and Heteroaryleneethinylenes†

E. Birckner,‡ U.-W. Grummt,*,‡ A. H. Göller,‡ T. Pautzsch,§ D. A. M. Egbe,§ M. Al-Higari,§ and E. Klemm§

Institut für Physikalische Chemie der Friedrich-Schiller-Universität Jena, Jena, Germany, and Institut für Organische und Makromolekulare Chemie der Friedrich-Schiller-Universität Jena, Jena, Germany

Received: February 12, 2001; In Final Form: May 3, 2001

The absorption spectra and the stationary and time-resolved emissions of a series of the title compounds are investigated. Various combinations of ethinylene, *p*-phenylene, biphenyl-4,4′-diyl, fluorenyl-2,7-diyl, 3- or 4-pyridyl, phenanthroline-3,8-diyl, 2,2′- bipyridine-5,5′-diyl, and 2,2′- bipyridine-4,4′-diyl molecular units allow a systematic structure variation, e.g., size of π system, type of aza-substitution, linear or angular chains. Most compounds are highly fluorescent. Radiationless deactivation via internal conversion and to a lesser extend intersystem crossing become efficient if forbidden states exist close to the strongly allowed $\pi\pi^*$ states (proximity effect) which can be traced back to a smaller size of the π system or reduced conjugation due to meta-linkages of heteroaromatic rings. Aza-substitution may change the deactivation behavior but it does insignificantly influence the absorption and fluorescence spectra. Replacing phenanthrene for 2,2′-bipyridine in the larger compounds does not alter the spectroscopic and the deactivation behaviors.

Introduction

The compounds 2,2-bipyridine and 1,10-phenanthroline are among the most important bidentate ligands in coordination chemistry.[1] These ligands deserve also particular interest as main chain building blocks of highly luminescent polymers which may also become interesting as electroluminescent as well as photoconductive materials. Balzani has recently stressed the importance of luminescent and redox-active polynuclear transition metal complexes.[2] Understanding the photophysics is one prerequisite for the chemical design of optimized luminescent polymers for practical application. From the point of view of technical processing it is necessary to modify these polymers by side chain substitution in order to enhance their solubility and film-forming property which may also affect their spectral and photophysical behavior. In a recent paper we have reported on the photophysical properties of fluorescent polymers with 1,10-phenanthroline-3,8-ylene and diethinylbenzene units, their low molecular weight model compounds, and related 2,2′-bipyridine analogues.[3] It turned out that there are very small differences between polymers as well as model compounds containing either 2,2-bipyridine or 1,10-phenanthroline units in the backbone, although one should expect that the differing structures (transoid and cisoid positions of the nitrogen atoms) and the restricted torsional motion should alter the spectral and photophysical properties.

This paper deals with the primary deactivation of photoexcited unsubstituted low molecular weight model compounds most of them may be regarded as different (unsubstituted) sections of polymers. The structural building units are 1,4-phenylene, 2,2′-bipyridine-5,5′-diyl, 1,10-phenanthroline-3,8-diyl, biphenyl-4,4-diyl, and fluorene-2,7-diyl which are linked by ethinylene bridges. In addition to the strictly linear rodlike compounds we have also included angularly linked isomers.

It is the purpose of this work to contribute to understanding the influence of structural variation on the absorption and emission properties of this class of compounds. In particular we have included compound with a systematical variation of the size of the π system, aza-substitution, and sterical fixation of the pyridine moieties.

The structures of the compounds are shown in Chart 1 together with their short codes used in this paper. Some of the compounds were synthesized for the first time.

Materials and Methods

Instrumentation. Molar absorptivities were determined in $CHCl_3$ and/or 1,4-dioxane (for HPLC, Baker) on a Perkin-Elmer UV/vis−NIR spectrometer Lambda 19.

All solvents used for the spectroscopic investigations were of spectroscopic grade (UVASOL, Merck: cyclohexane (CH), methylcyclohexane (MCH), toluene, diethyl ether, acetonitrile (ACN), ethanol (EtOH), and tetrahydrofuran (THF)).

Absorption spectra at room temperature were recorded on a LAMBDA 16 spectrophotometer (Perkin-Elmer). Fluorescence and phosphorescence emission and excitation spectra were measured with an LS50B luminescence spectrometer (Perkin-Elmer). Fluorescence quantum yields were calculated relative to quinine sulfate (purum, Fluka) in 0.1 N H_2SO_4 (pro analysi, Laborchemie Apolda) used as a standard ($\Phi_f = 0.55$) according to ref 4. The absorbance at the excitation wavelength was kept below 0.05 for the samples and the reference.

The ratio of the phosphorescence and fluorescence quantum yields was obtained from the integrals of the well separated corrected fluorescence and emission spectra at 77 K. For this measurements the single photon counting spectrometer CD900 (Edinburgh Instruments) was used in the steady-state mode (excitation source: Xe-lamp 450 W).

The instrument was also used in the time correlating mode for all kinetic investigations. The excitation source was a

† This work was presented at the PP2000 in Costa do Estoril, Portugal, honoring Professor Ralph Becker's contributions.

‡ Institut für Physikalische Chemie der Friedrich-Schiller-Universität Jena.

§ Institut für Organische und Makromolekulare Chemie der Friedrich-Schiller-Universität Jena.

10.1021/jp010546n CCC: $20.00
Published on Web 06/30/2001

CHART 1

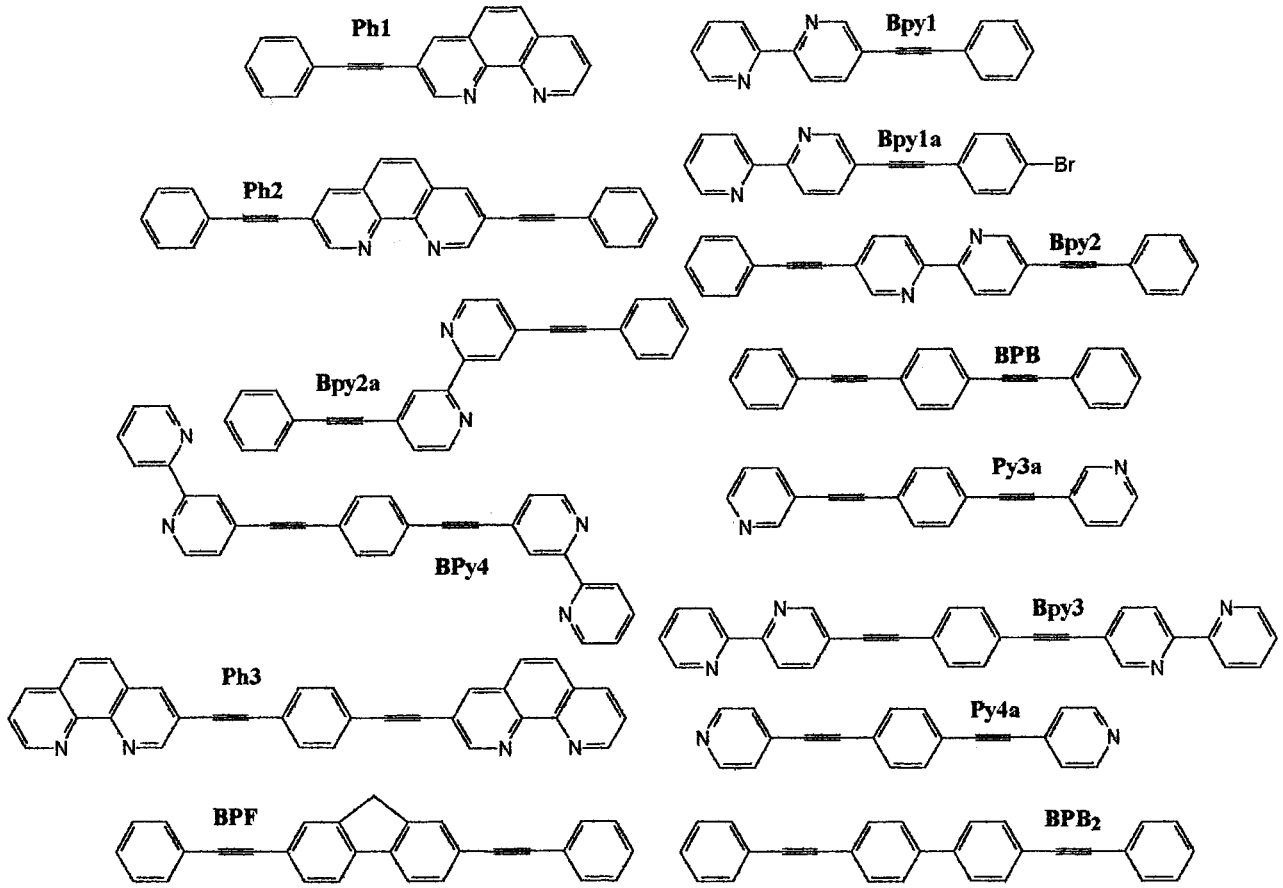

hydrogen filled nanosecond flashlamp giving a instrument response pulse of 1.3 ns fwhm. Polarizers with a vertical orientation on the excitation side and a 55° (magic angle) orientation on the emission side were used to avoid polarization effects. Decay curves were accumulated until 10^4 counts in the maximum with at least 10^3 occupied channels. To determine rotational relaxation times directly from kinetic measurements, the decay curves were measured with a parallel and a perpendicular oriented analyzer.

To calculate the fluorescence lifetime and the rotational relaxation time the LEVEL 1 (up to 4 exponentials) and LEVEL 2 (spherical rotor) packages implemented in the Edinburgh Instruments software were used. (The analysis makes use of the iterative reconvolution technique and the Marquardt fitting algorithm.) Plots of weighted residuals and of the autocorrelation function and values of reduced residuals χ^2 were used to judge the quality of the fit. χ^2 larger than 1.3 were not accepted. The experimental errors of the measured values given in the tables are $\lambda_{a,f} = \pm 2$ nm, $\epsilon = \pm 10\%$, $\Phi_f = \pm 10\%$ for $\Phi_f > 0.5$ and $\pm 20\%$ for $\Phi_f < \pm 0.5$, $\tau = < 100$ ps, $r = \pm 0.02$. In the case of structured spectra, the subbands of maximal intensity are italicized.

Transient absorption experiments in the microsecond time scale were performed with a conventional flash photolysis apparatus.[5] Solutions were deoxygenated by bubbling nitrogen through the samples. Schott glass filters UG2 were used for excitation.

Quantum Chemical Calculations. The position of spectral transitions and oscillator strengths were calculated by the INDO1(S) method using the ARGUS program.[6] Molecular geometries were obtained from ab initio DFT calculations using the GAUSSIAN 98 package[7] (b3lyp /6-31+g(d)).

Synthesis. Five compounds investigated in this work have hitherto not been described the preparation of which is briefly outlined.

Information on synthetic procedures can be found in the references given: **Bpy1**,[8] **Ph2**,[9,10] **Bpy2**,[11] **Bpy2a**,[11] **Bpy3**,[12] **Py3a**,[11] **Bpy4**,[13] **Py4a**,[11] and **BPB**.[14]

Ph1. To a thoroughly deoxygenated mixture of 25 mL diisopropylamine and 50 mL of dry toluene, 518 mg (2 mmol) of 3-bromo-1,10-phenanthroline, 255 mg (2.5 mmol) of phenylacetylene, 15 mg of CuI, and 92 mg of $Pd(PPh_3)_4$ were added, and the solution was stirred for 24 h at 70 °C. The precipitated diisopropylammonium bromide was filtered off. The solution was evaporated to dryness and the residue was dissolved in chloroform. The solution was washed with water, dried over $MgSO_4$, and concentrated under reduced pressure. After purification by column chromatography (silica gel, hexane/ethyl acetate 1:1), 190 mg of a pale yellow product was obtained (34%), fp = 175−177 °C. ^{1}H NMR (250 MHz, $CDCl_3$): δ = 7.37 (m, 6 H_{ph}), 7.60 (m, 4 H_{ph}) 7.76 (d, 2 H_{phen}), 8.35 (d, 2 H_{phen}, ^3J = 8.30 Hz), 9.25 (d, 2 H_{phen}). ^{13}C NMR (62 MHz, $CDCl_3$): δ = 86.36, 94.05, 119.84, 122.43, 125.38, 127.90, 128.54, 129.61, 131.76, 136.05, 138.03, 144.37, 145.92, 150.66, 151.23, 152.48. IR (KBr): 2209 (disubstituted −C≡C−) cm^{-1}. Anal. Calcd for $C_{20}H_{12}N_2$ (280.31): C, 85.70; H, 4.31; N, 9.99. Found: C, 85.37; H, 4.10; N, 9.52.

Bpy1a. $Pd(PPh_3)_4$(96 mg, 8.3×10^{-5} mol, 2 mol %) and CuI (16 mg, 8.3×10^{-5} mol, 2 mol %) were given to a mixture of 5-ethinyl-2,2'-bipyridine (500 mg, 2.8 mmol), p-iodobromobenzene (1.2 g, 4.2 mmol), and diisopropylamine (30 mL) in dried THF (70 mL). The reaction mixture was stirred at 40 °C for 14 h. It was filtered to remove the inorganic compounds. The precipitate was washed with chloroform and both filtrates

TABLE 1: Photophysical Data in Dioxane at Room Temperature

	λ_a, nm	ϵ, M^{-1} cm^{-1}	λ_f, nm	Φ_f	τ, ns	r
Ph1	*315*/332	31 200	362/*379*	0.025	2.0[c]	0.18
Bpy1	*317*/335	34 000	346/*364*	0.23	0.30	0.12
Bpy1a	*319*/338	44 700[a]	350/*366*	0.31	0.32	0.15
Ph2	*338*/357	47 000[b]	372/*392*	0.20	2.13	0.049
Bpy2	*341*	64 000	*375*/394	0.98	0.76	0.12
Bpy2a	*301*/319	52 000[a]	360	<0.01	not determined	not determined
Ph3	*352*/370	not determined	*377*/397	0.81	0.61	0.17
Bpy3	*348*/368	49 400	*377*/400	1	0.60	0.17
Py3a	*320*/340	48 900	*346*/362	1	0.62	0.086
Bpy4	*323*/343	53 000[a]	*352*/369	1	0.50	0.15
Py4a	*318*/337	40 500	*345*/362	0.60	0.40	0.12
BPB	*320*/341	62 000	*347*/363	0.90	0.64	0.082
BPF	*347*/362	83 600	*368*/387	1	0.67	0.13
BPB_2	*308*	52 500	341/*366*/383	0.72	0.51	0.12

[a] ϵ determined in $CHCl_3$. [b] ϵ determined in toluene. [c] Mean value, determined by $\langle\tau\rangle = 1/(\phi_1/\tau_1 + \phi_2/\tau_2)$ with $\tau_1 = 1.4$ ns, $\tau_2 = 4.4$ ns, $\phi_1 = 0.9$, $\phi_2 = 0.1$.

were dried over $MgSO_4$, evaporated to dryness and chromatographed with hexane/ethyl acetate (v/v: 1:2) on silica gel, yielding 660 mg of pale yellow powder (71.4%), mp = 148 °C. ^{1}H NMR (400 MHz, $CDCl_3$): δ = 8.78 (s, 1 H), 8.68 (d, ^4J = 3.9 Hz, 1 H), 8.41 (d, ^3J = 8.2 Hz, 2 H), 7.91 (dd, ^3J = 8.2 Hz, ^4J = 2.1 Hz, 1 H), 7.82 (td, ^3J = 7.8 Hz, ^4J = 1.7 Hz, 1 H), 7.50 (d, ^3J = 8.6 Hz, 2 H), 7.41 (d, ^3J = 8.4 Hz, 2 H), 7.31 (td, ^3J = 4.9 Hz, ^4J = 1.6 Hz, 1 H). ^{13}C NMR (100 MHz, $CDCl_3$): δ = 151.52, 149.07, 139.31, 137.08, 133.03, 131.69, 123.96, 123.08, 121.45, 121.38, 120.36, 119.96, 92.36, 87.37. Anal. Calcd for $C_{18}H_{11}N_2Br$ (335.21) (%): C, 64.50; H, 3.31; N, 8.36; Br, 23.84. Found (%): C, 64.59; H, 3.51; N, 8.36; Br, 23.61.

Ph3. One hundred forty milligrams of $Pd(PPh_3)_4$ and 23 mg of CuI were added to a mixture of 573.2 mg (2.2 mmol) of 3-bromo-1,10-phenanthroline, 126.2 mg (1.0 mmol) of diethinylbenzene, 15 mL of diisopropylamine, and 40 mL of toluene under argon at room temperature. The mixture was stirred under argon at reflux for 24 h. After cooling to room temperature an excess of methanol was added. The yellow precipitate was filtered off and reprecipitated from toluene with methanol yielding 380 mg (40%) of a yellow product, fp > 270 °C. ^{1}H NMR (250 MHz, DMSO): δ = 9.11, 9.18, 8.69, 8.45, 8.00, 7.72 (7 H_{phen}), 7.32 (4 H_{ph}). IR (KBr): 2211 (disubstituted −C≡C−) cm^{-1}.

BPF. Five hundred twelve milligrams of 2,7-dibromofluorene (1.58 mmol), 110 mg of $Pd(PPh_3)_4$ (4 mol %), and 18 mg of CuI were dissolved under argon in a deoxygenated solution of 15 mL of diisopropylamine in 40 mL of toluene. Phenylacetylene (356.6 mg, 3.5 mmol) were added dropwise, and the mixture was stirred at 70−80 °C for 24 h. After it was cooled to room temperature, the reaction mixture was given dropwise under stirring to 300 mL of methanol. The solid precipitate was collected after 15 min stirring, dissolved in 20 mL of toluene, and filtered through a 4 cm layer of silica gel on a glass frit. After the solvent was evaporated, the product was precipitated twice from toluene solution by addition of methanol yielding 290 mg (79%) of a light yellow solid, fp = 237 °C. ^{1}H NMR (250 MHz, $CDCl_3$): δ = 3.90 (s, 2 H, $-CH_2-$), 7.31 (m, 6 H, $H_{fluorene}$), 7.53 (t, 6 H, H_{Ph}), 7.71 (t, 4 H, H_{Ph}). ^{13}C NMR (100 MHz, $CDCl_3$): δ = 36.53 ($-CH_2-$), 89.77, 90.05 (−C≡C−), 119.98, 121.96, 123.51, 128.10, 128.13, 130.66, 131.55, 141.22, 143.51. IR (KBr): 2203 (disubstituted −C≡C−) cm^{-1}. Anal. Calcd for $C_{29}H_{18}$ (366.46): C, 95.05; H, 4.95. Found: C, 94.75; H, 4.96.

BPB_2. Compounds 4,4′-dibromobiphenyl (2 g, 6.41 mmol), $Pd(PPh_3)_4$ (73.5 mg, 6.125×10^{-3} mmol, 1 mol %), and CuI-(24.5 mg, 12.65×10^{-3} mmol, 2 mol %) were given to a degassed mixture of phenylacetylene (2.29 g, 22.4 mmol), triethylamine (10 mL), and toluene (60 mL). The reaction mixture was heated for 8 h under reflux and under argon. It was poured in an excess of methanol after cooling, and a precipitate was obtained. The precipitate was chromatographed on a silicagel column with hexane/THF: 3 /1 as eluent. A white substance was obtained [1.5 g (66%)] , mp = 196−198 °C. ^{1}H NMR (400 MHz, $CDCl_3$): δ = 7.33−7.35 (m, 6 H), 7.44−7.46 (m, 2 H), 7.51−7.59 (m, 10 H). ^{13}C NMR (100 MHz, $CDCl_3$): δ = 89.09, 90.35 (−C≡C−), 121.93−140.03 (phenyl C's). IR (KBr): 2209 cm^{-1} (−C≡C−). Anal. Calcd for $C_{28}H_{18}$ (354.45): C, 94.88; H, 5.11. Found: C, 94.75; H, 5.23.

Results and Discussion

Absorption. The absorption of the selected compounds recorded in the UV−vis region down to 250 nm is characterized by one or two intense bands below 400 nm. They are weakly structured at room temperature with a shoulder which is 1500−1800 cm^{-1} bathochromically shifted with respect to the long wavelength maximum. This shoulder becomes the long wavelength maximum of a prominent vibrational structure at liquid nitrogen temperature.

The position of the absorption and fluorescence bands exhibits only a minor dependence on the solvent. Spectra and photophysical data were determined for all compounds in dioxane as a solvent. A few compounds were also investigated in solvents of different polarity. Figures 1, 2, 4, and 5 show absorption spectra recorded in dioxane at room temperature. The absorption maxima and the location of the shoulder of the longest wavelength band together with the molar absorptivities are given in Table 1.

According to their absorption behavior the compounds may be divided up into the following classes:

(i) The "small compounds" consisting of one phenylethinyl unit and one 1,10-phenanthroline or 2,2′-bipyridine moiety (**Ph1**, **Bpy1**, and **Bpy1a**) absorb at about 315 nm with molar absorptivities around 30 000 M^{-1} cm^{-1}.

(ii) The compounds consisting of three phenyl(ene) rings (**BPB**) or one phenylene ring and two pyridyl units connected by ethinylene linkages (**Py4a** and **Py3a**) absorb nearly at the same wavelength; however, they exhibit a larger absorptivity in the range of 40 000−60 000 M^{-1} cm^{-1}.

(iii) Compounds with the larger heteroaromatic building blocks 2,2′-bipyridine (**Bpy2**) or 1,10-phenanthroline (**Ph2**) in the linear backbone absorb at significantly longer wavelengths,

the molar absorptivity being not increased. A further enhancement of the π system (**Bpy3** and **Ph3**) brings about only a minor bathochromic shift of the absorption.

Compounds with the phenanthroline subchromophore show a significantly enhanced absorption in the 250−280 nm region ($\epsilon > 30\,000$ M^{-1} cm^{-1}) by comparison with those containing the bipyridine subchromophore ($\epsilon < 20\,000$ M^{-1} cm^{-1}). Obviously, this is a local transition in accord with the larger absorption of phenanthroline in this region (phenanthroline, $\epsilon_{263\,nm} = 26\,500$ M^{-1} cm^{-1}; bipyridine, $\epsilon_{278\,nm} = 14\,000$ M^{-1} cm^{-1} [15]).

From a comparison of the linear compounds (**Bpy2** and **Bpy3**) with the isomeric angular ones (**Bpy2a** and **Bpy4**) the influence of the linkage type (*meta*-hetero-arylene or *para*-hetero-arylene unit in the backbone) on the extent of conjugation becomes obvious. The absorption of **Bpy2a** is only slightly red-shifted in comparison with tolane ($\lambda_{max} = 295$ nm, $\epsilon = 29\,000$ M^{-1} cm^{-1});[15] however, it is significantly more intense. Evidently, meta-linking distorts π-conjugation efficiently. Thus, the absorption can be interpreted as a superimposition of two tolane units.

Bpy4 absorbs at a significantly shorter wavelength than its isomer **Bpy3**, and it differs only slightly from **Py4a** which demonstrates the negligible conjugative effect of the angularly linked pyridyl units. We exclude nonplanarity of the bipyridine units as a reason for conjugation interruption in accord with our recent theoretical results.[17]

A noncoplanar arrangement of two directly connected aromatic rings due to steric hindrance causes the hypsochromic shift and the featureless structure of the long-wavelength absorption band observed with the biphenyl analogue (**BPB_2**) of **Bpy2**. It becomes obvious from a comparison with the fluorene derivative **BPF** where the sterical hindrance of the biphenyl unit is excluded that we have indeed an essentially steric rather than an electronic effect. The absorption spectra of **Bpy2** and **BPF** are nearly identical as are their fluorescence spectra to be discussed below.

Fluorescence. The fluorescence spectra of the investigated compounds excited at the longest wavelength absorption maximum are given in Figures 1−5. The fluorescence excitation spectra coincide well with the corresponding absorption spectra. The positions of the fluorescence maxima, fluorescence quantum yields, lifetimes, and emission anisotropies together with absorption data are contained in Table 1. Data were obtained at room temperature in dioxane as a solvent. Photophysical data of the compounds **Bpy2**, **Bpy2a**, **Bpy3**, **Py3a**, **Py4a**, and **BPB** in toluene solution were recently reported by us.[11]

With the exception of **Ph1** and **Bpy2a**, all compounds selected are highly fluorescent already at room temperature. The fluorescence spectra are clearly structured and resemble each other. The vibrational spacings of the main progressions are in the typical region of the aromatic C−C stretching modes 1300 to 1500 cm^{-1}. There are no indications of structural features attributable to −C≡C− streching modes.

The Stokes shifts of the highly fluorescent derivatives are small and amount from 1500 to 3000 cm^{-1}. Larger Stokes shifts were obtained with the derivatives of lower fluorescence quantum yields. At 77 K the difference of the 00 transitions of absorption and fluorescence (the anomalous Stokes shift) becomes minimal (about 300 cm^{-1}, cf. Table 4) which indicates only small geometry changes between S_0 and S_1 states in the rigid solvent matrix.

Special interest deserves the elucidation of the *fluorescence kinetics*. For diphenylacetylene the existence of different electronic states lying close to one another is discussed which result in a S_2 fluorescence.[18] In ref 19, which refers to 9,10-di(phenylethinylen)anthracene, the existence of different conformers with coplanar and noncoplanar arrangements of the anthracene and phenyl nuclei is assumed.

In our compounds, especially in the larger systems with two triple bonds, the existence of different emitting species is not to be excluded. Fluorescence decay curves of all compounds excited in the long wavelength absorption maximum were measured in dioxane at room temperature. A few compounds were measured also in other solvents and at lower temperatures. With the exceptions of **Ph1** and **Ph2** in toluene at room temperature and in ethanol at 77 K the fluorescence decay curves are monoexponential with short lifetimes around 0.5 ns. Monoexponential decay curves were also obtained for all other investigated compounds (**Bpy1**, **Bpy1a**, **BPB**, **Bpy2**, **Py4a**, and **Py3a**) with excitation in the long wavelength shoulder and measured at different emission wavelengths. Within the given time resolution of 50−100 ps, the lifetimes are independent of both the excitation and the emission wavelength at room temperature. From these results there are no indications for different emitting species or a dual fluorescence. The fluorescence lifetimes are given in Table 1.

Table 2 shows the radiative and nonradiative rate constants obtained from the experimental lifetimes and the quantum yields

TABLE 2: Rate Constants in Dioxane at Room Temperature

	Φ_f/τ, ns^{-1}	k_{nr} [a], ns^{-1}	k_f (SB)[b], ns^{-1}	Φ_f/τ /k_f (SB)
Ph1	0.02[c]	0.75	0.37	0.054
Bpy1	0.77	2.6	0.66	1.2
Bpy1a	0.97	2.2	0.86	1.1
Ph2	0.10	0.40	0.60	0.17
Bpy2	1.3	<0.1	0.96	1.4
Bpy2a			0.8[d]	
Ph3	1.3	0.31		
Bpy3	1.7	<0.1	0.90	1.8
Py3a	1.6	<0.1	0.98	1.6
Bpy4	2.0	<0.1	1.2	1.7
Py4a	1.5	1.0	0.79	1.9
BPB	1.4	0.16	0.92	1.5
BPF	1.5	<0.1	1.3	1.1
BPB_2	1.4	0.55	1.1	1.3

[a] $k_{nr} = (1 - \Phi_f)/\tau$. [b] According to ref 18; ϵ values from Table 1. [c] Determined with the mean lifetime (Table 1) [d] From ref 10, solvent toluene.

TABLE 3: Results of Time Resolved Polarization Measurements (τ, ρ, r_0) Compared with Calculated Rotational Relaxation Times (ρ_{Calc}) and Steady-State Emission Anisotropies r (cf. Table 1) in Dioxane at Room Temperature

code	a[a] / b	ρ_{calc}[b], ns	ρ, ns	τ, ns	r_0	r_{tr}[c]	r
Ph2	1.14 / 0.29	0.48	0.43	2.13	0.34	0.057	0.049
Bpy2	1.14 / 0.22	0.37	0.48	0.76	0.37	0.14	0.12
Ph3	1.36 / 0.29	0.68	0.60	0.61	0.38	0.19	0.17
Bpy3	1.37 / 0.22	0.52	0.52	0.60	0.39	0.18	0.17
BPB	0.94 / 0.22	0.25	0.22	0.67	0.26	0.064	0.082
BPF	1.13 / 0.265	0.44	0.46	0.67	0.34	0.14	0.13

[a] Long and short molecular halfaxes a and b in nanometer. [b] Calculated by $\rho_{calc} = 4\eta\pi a^2 b/3kT$, η(dioxane, 293 K) = 1.24 cP. [c] Calculated by $r_{tr} = r_0/(1 + \tau/\rho)$ (Perrin).

TABLE 4: Fluorescence and Phosphorescence at 77 K. Solvent: EtOH

code	λ_{ex}, nm	λ_f, nm	λ_p, nm	Φ_p/Φ_f	Φ_p[b]
Ph1	340/*344*/355	359/367/*377*/397	*488*/516/528/546	0.22	<0.02
Bpy1	325/*340*	*345*/363	505/545	0.025	<0.025
Bpy1a	331/*344*	*347*/366	513/548	0.075	<0.075
Ph2	350/*370*	*374*/397	515/534/560	0.05	<0.05
Bpy2	282/352/*371*	*375*/397	*514*/545	≪0.01	≪0.01
Bpy2a	302/*310*/321	330/*345*	*456*/482/509	not determined	not determined
Ph3	349/357/362/*377*	*380*/398/416	*541*	≪0.01	≪0.01
Bpy3	349/356/*376*	*379*/398/414	ca. 550	≪0.01	≪0.01
BPB[a]	324/330/335/*349*	*351*/363/369/380			
Py4a	324/330/335/*349*	*350*/364/370/379			

[a] Spectra measured in the solvent MCH at 123 K. [b] Data estimated with $\Phi_f \approx 1$ at 77 K for all compounds with the exception of **Ph1**: $\Phi_f(77\ K) \approx 0.05$.

together with the radiative rate constants determined from the Strickler/Berg equation.[20]

The radiative rate constant of the most compounds obtained from Φ_f/τ is large and indicates a strongly allowed emission moment. The values Φ_f/τ and the radiative rate constant k_f(SB) calculated after Strickler/Berg, which reflects mainly the absorption transition moments show a reasonable agreement. However, the emission transition moment is in general slightly larger. The reason for this is, evidently, the enhanced π conjugation in the emitting S_1 state due to smaller deviations from planarity.

The disagreement in the case of the phenanthroline derivatives and the nonradiative deactivation will be discussed below.

The *emission anisotropy* of the different compounds was investigated in order to get experimental information on the direction of the transition moments of absorption and emission. The limiting anisotropy r_0 obtained from time-resolved polarization measurements is of particular interest for the investigation of energy transfer in polymers containing bipyridyl or phenanthroline units. An anisotropy well above zero measurable already in the low viscous solvent dioxane is typical for these rodlike compounds. Data of emission anisotropies from steady-state measurements are included in Table 1. Table 3 contains the results of time-resolved polarization measurements.

The measured rotational relaxation times correspond to the dimension of the rodlike molecules and characterize the depolarizing movement as the torsion perpendicular to the long molecular axis containing the transition moment. Furthermore, the emission anisotropies r calculated from the data of the time-resolved measurements (τ, ρ, and r_0) show a close agreement with the anisotropies from steady-state measurements. Obviously, the depolarizing rotation is well described within the experimental errors by the simple Stokes−Einstein model.

All compounds, as mentioned above, do exhibit only minor *solvent dependence* of the spectra. Also, the quantum yield and lifetime of the highly fluorescent compounds vary with the solvent just slightly exceeding the limits of error. The solvent dependent properties of **Ph1**, **Bpy1**, **Ph2**, **Bpy2**, **Bpy3**, **Ph3**, and **BPB** were studied in more detail.

For **Bpy2** the quantum yields and lifetimes vary in solvents of different polarity from 0.89 (EtOH) to 1 (THF, dioxane) and from 0.67 ns (CH) to 0.80 ns (EtOH, ACN), respectively. Similarly, for **Bpy3** the quantum yields vary from 0.76 (toluene) to 1 (dioxane) and the lifetimes range from 0.53 ns (toluene) to 0.62 ns (EtOH). **BPB** gives quantum yields from 0.79 (toluene) to 0.90 (dioxane) and lifetimes from 0.59 ns (toluene) to 0.69 ns (MCH).

Generally, the phenanthroline derivatives show a more pronounced solvent dependence of the quantum yields and lifetimes which will be dicussed below.

As expected, the fluorescence quantum yield of all compounds increases with decreasing temperature. Of course, the

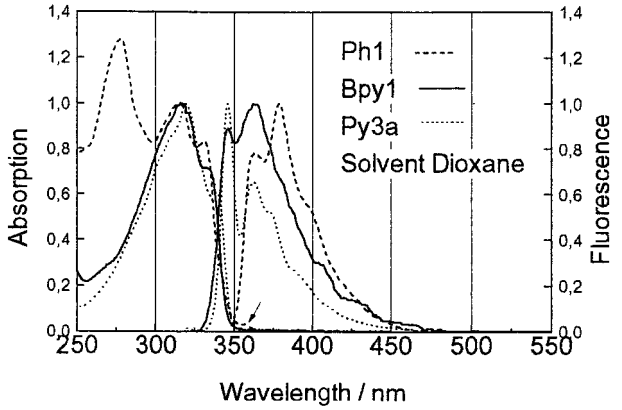

Figure 1. Absorption and fluorescence spectra of **Ph1**, **Bpy1**, and **Py3a** in dioxane at room temperature.

fluorescence quantum yields and lifetimes of the highly fluorescent compounds vary only slightly with temperature below room temperature. At higher temperatures a moderate decrease is observed. As an example, with increasing temperature between 10 and 70 °C the fluorescence quantum yield of **Bpy2** in EtOH drops from 0.96 to 0.81. The quantum yield of **Ph2** in EtOH ($\Phi_f = 0.52$ at room temperature) shows a stronger temperature dependence: Φ_f decreases by nearly 50% from 0.56 to 0.31 between 10 and 70 °C. From a simple kinetic model which assumes one thermally activated radiationless deactivation channel (k_0* exp($-E_a/RT$)) competing with fluorescence (k_f) and temperature independent radiationless deactivation (k_d) one obtains for the temperature dependence of the reciprocal fluorescence quantum yield:

$$1/\Phi_f = 1 + k_d/k_f + k_0/k_f \exp(-E_a/RT)$$

The experimental fluorescence data of **Ph2** fit perfectly to this model. Nonlinear regression yields $E_a = (24.8 \pm 0.3)$kJ/mol, $k_d/k_f = 0.52 \pm 0.1$, and $k_0/k_f = 1.0 \pm 0.1$.

At low temperatures the fluorescence spectra are clearly structured. An example is given in Figure 3 showing the fluorescence excitation and emission spectra of **Bpy2** and **Ph2** at 77 K. Structured low-temperature spectra were obtained also with **Ph1**, **Bpy1**, **Bpy1a**, **Bpy3**, **Py4a**, and **BPB**.

Table 4 contains wavelengths of fluorescence and phosphorescence emission maxima, and of fluorescence excitation spectra together with relative phosphorescence yields, measured at 77 K. Phosphorescence (recorded in the phosphorescence mode of the LS50B) was identified by the comparison of the phosphorescence excitation spectra with the fluorescence excitation spectra. For **Ph1**, **Bpy1**, **Bpy1a**, **Py4a**, and **BPB** both the fluorescence and phosphorescence spectra are independent of the excitation wavelength. In the cases of **Ph2**, **Bpy2**, **Ph3**, and

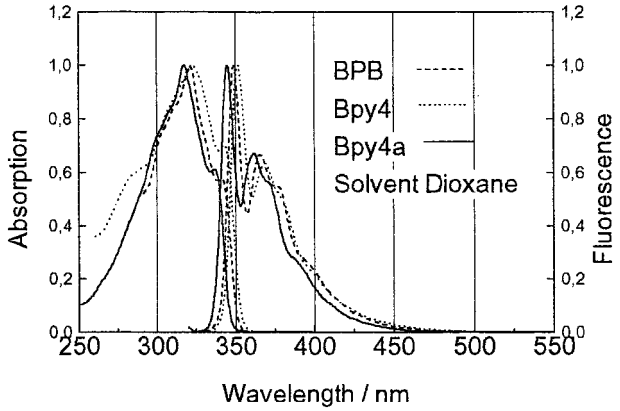

Figure 2. Absorption and fluorescence spectra of **BPB**, **Bpy4**, and **Bpy4a** in dioxane at room temperature.

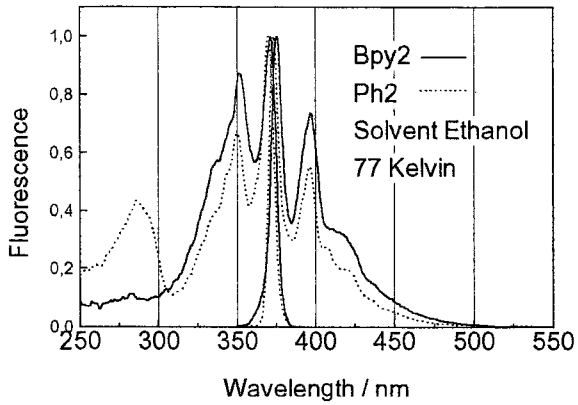

Figure 3. Fluorescence excitation and fluorescence emission spectra of **Bpy2** and **Ph2** in ethanol at 77 K.

Bpy3 we found again fluorescence spectra independent of the excitation wavelength. However, excitation with shorter wavelengths results in additional phosphorescence bands which might, tentatively, originate from aggregates, nonequilibrium conformers, site effects, or even from small amounts of impurities like metal complexes.

At 77 K the fluorescence quantum yields of **Bpy2**, **Ph3**, **Bpy3**, **Py4a**, and **BPB** are expected to approach unity and, consequently, the phosphorescence quantum yields are smaller than 1%.

For the compounds **Ph1**, **Bpy1**, and **Bpy1a**, the upper limit of the phosphorescence quantum yields is 10%, as can be estimated from a comparison of the fluorescence and phosphorescence intensities at 77 K assuming the fluorescence quantum yields to be unity. The real values should be two to three times smaller.

We shall now discuss the fluorescence properties of the particular compounds in more detail and compare them to each other.

Figure 1 shows the fluorescence spectrum of the "small compound" **Bpy1** together with the absorption spectra, which is compared with the bromo-substituted compound **Bpy1a** (not displayed), the analogous 1,10-phenanthroline compound **Ph1** and **Py3a**. **Bpy1** is moderately fluorescent; the fluorescence spectrum is mirror-symmetric to the absorption spectrum, and the radiative rates k_f (SB) and Φ_f/τ coincide well. At 77 K in ethanol and in diethyl ether **Bpy1** exhibits an intense well structured fluorescence with a minimal Stokes shift as well as a phosphorescence peaking at 505 nm (00 transition). Hence, the S_1 state deactivates via temperature-dependent internal conversion (ic) and intersystem crossing (isc).

We have also investigated the bromo-substituted compound **Bpy1a** in order to answer the question in how far the bromo substituent which is a terminating atom in the polymers gives rise to a possible reduction of the fluorescence quantum yield due to enhanced isc.

The results show, however, that bromo substitution seems even to decrease the nonradiative deactivation rate ($k_{ic} + k_{isc}$), cf. Table 2. The increase of the phosphorescence quantum yield of **Bpy1a** in comparison to **Bpy1** at 77 K indicates either an increase of the phosphorescence rate constant k_p or, in the case of enlarged heavy atom induced isc, a reduced internal conersion rate k_{ic}.

Absorption and fluorescence spectra of **Bpy1a** are essentially identical with those of **Bpy1**.

Although the longest wavelength absorption bands of **Bpy1** and **Ph1** resemble each other very closely in structure and intensity and, hence, similar radiative rates are calculated from the Strickler/Berg equation (cf. Table 2), both compounds differ considerable in their fluorescence properties. This becomes evident mostly from the drastically reduced fluorescence quantum yield and from the biexponential decay kinetics together with the bathochromically shifted fluorescence band of **Ph1**. Although the calculation of a radiative rate constant is, in a strict sense, impossible in the case of a nonexponential decay, we can estimate a radiative rate constant already from mean fluorescence lifetime which is 1 order of magnitude smaller than the value obtained after Strickler/Berg. Also the increased fluorescence lifetime indicates a weaker transition moment. Obviously, the absorption at 315 nm ($\epsilon = 31\ 200\ M^{-1}\ cm^{-1}$) is not the $S_0 \rightarrow S_1$ transition. According to the radiative rate constant Φ_f/τ we may assign the preband at 358 nm (indicated by an arrow in Figure 1) to the $S_0 \rightarrow S_1$ transition. The molar absorptivity of this band is less than $1500\ M^{-1}\ cm^{-1}$ which results, after Strickler/Berg, in a radiative rate constant in the order of the Φ_f/τ value of $0.02\ ns^{-1}$. Low-lying $n\pi^*$ transitions (320−340 nm) are reported for 1,10-phenanthroline with absorptivities from 90 to $600\ M^{-1}\ cm^{-1}$.[15]

At 77 K **Ph1** (solvent EtOH) exhibits a structured fluorescence with 2-fold higher intensity compared with room temperature and an intense phosphorescence with a maximum at 488 nm (Table 4). Thus, we conclude that isc is effective as an deactivation channel with **Ph1** promoted presumably by the proximity of an $n\pi^*$ excited-state according to the well-known El-Sayed rules.[16]

Not only is the investigation of the photophysics of **Ph1** made more difficult by the low fluorescence quantum yield, but it is further complicated by the occurrence of an additional absorption and fluorescence in nonpolar aprotic and in polar aprotic solvents. Since this species is not observed in aromatic or protic solvents, we assign it to an aggregate the formation of which is prevented by strong solvation or hydrogen bridge formation. Further investigations are necessary to fully understand the photophysics of **Ph1**.

Joshi et al.[21] have published the absorption and fluorescence spectra of a methyl-substituted **Ph1**, showing that the spectra are nearly unaffected by the substituent and the fluorescence quantum yield was found to be 10-fold larger.

The coincidence of the absorption and fluorescence maxima of **Py3a** and **Bpy1** is surprising taking into account the different molecular structures. Both compounds differ considerably in the amount of their transition moments for absorption and emission, as well as in the deactivation which is essentially radiative with **Py3a**. Substitution of a phenyl ring by a pyridyl group in the chain has no effect on the spectral behavior (3- or

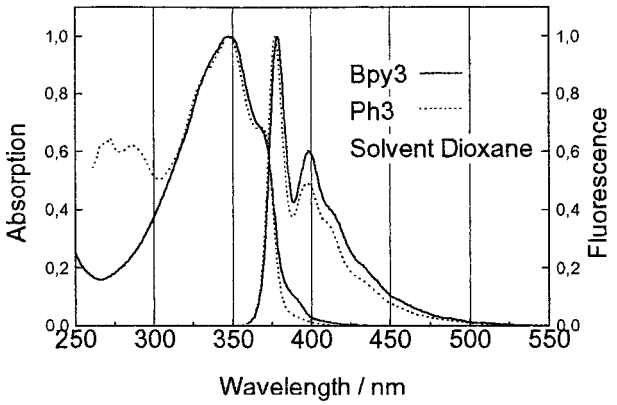

Figure 4. Absorption and fluorescence spectra of **Bpy3** and **Ph3** in dioxane at room temperature.

4-pyridyl: **Py3a**, **Py4a**). Figure 2 shows the spectra of the compounds **BPB** and **Py4a** together with the angular species **Bpy4**. As already mentioned above, the outer 2-pyridyl rings in **Bpy4** attached in meta-positions to the ethinylene linkages exhibit only a minor influence on both the spectral properties and the deactivation behavior. It is obvious from the spectra that not only the band position but also their shapes are nearly identical. These compounds show large fluorescence quantum yields and small lifetimes resulting in large radiative and small nonradiative rates (cf. Tables 1 and 3). Remarkable nonradiative deactivation is observed with **Py4a**.

A further enlargement of the π system results in a considerable bathochromic shift of the absorption and the fluorescence. Figure 3 shows the fluorescence and the fluorescence excitation spectra of the bipyridine- and the phenanthroline compounds **Bpy2** and **Ph2**, recorded in ethanol at 77 K. The excitation spectra again coincide with the absorption spectra obtained under identical conditions. The spectra show a distinctive vibrational structure which was also observed with **Bpy1** and **Bpy3** at 77 K. Again we observe with **Ph2** the local transition due to the phenanthroline subchromophore. The close similarity of the band shapes and the nearly perfect coincidence of the maxima in the spectra of **Bpy2** and **Ph2**, however, is unexpected if one considers both the restriction of torsional motion by the ethinylene bridge in **Ph2** and the different spatial arrangement of the N atoms, whereas **Bpy2** has no permanent dipole moment due to ist transoid equilibrium conformation **Ph2** is a dipole molecule.

Very similar results were obtained from a comparison of **Bpy3** and **Ph3** which again differ from each other merely by the substitution of bipyridine for phenanthroline, see Figure 4. The positions of the absorption and fluorescence bands coincide and the band shapes differ insignificantly. Whereas the enlargement of the π system when passing from **Bpy2** to **Bpy3** or from **Ph2** to **Ph3** exhibits only a minor influence on the spectra, there is, nevertheless, a significant difference concerning the deactivation between the bipyridine and phenanthroline derivatives. The bipyridine compounds show fluorescence quantum yields close to unity independent of the nature of the solvent. The lifetimes are close to 0.6 ns. The radiative deactivation rates calculated by various methods coincide reasonably, with $k_f(SB) < \Phi_f/\tau$ for all compounds of this type.

Among the phenanthroline derivatives the properties of **Ph2** and **Ph3** differ from each other. The fluorescence quantum yields and the lifetimes of **Ph2** depend on the solvent as also observed to a lesser extend with the fluorescence spectra.[21] In toluene the decay follows a biexponential rate law. At 77 K an easily detectable phosphorescence is observed. The dependence

TABLE 5: Solvent Dependence of the Deactivation of Ph2 at Room Temperature

solvent	λ_a, nm	λ_f, nm	Φ_f	τ, ns	k_f, ns^{-1}	$k_{nr}{}^a$, ns^{-1}
CH	337	*367*/390	0.11	1.92	0.055	0.45
toluene	340	*373*/398	0.10	0.72	0.15	1.19
dioxane	338	372/*392*	0.20	2.1	0.10	0.38
THF	341	*374*/395	0.19	1.23	0.15	0.66
ACN	338	*374*/391	0.33	2.83	0.12	0.24
EtOH	343	*376*/393	0.56	2.24	0.25	0.20

^{a} $k_{nr} = (1 - \Phi_f)/\tau$.

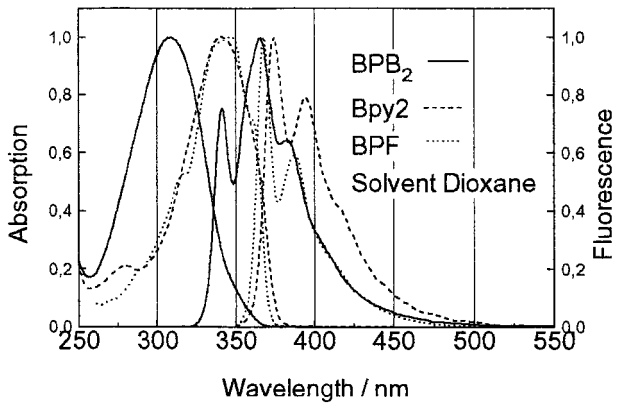

Figure 5. Absorption and fluorescence spectra of **BPB$_2$**, **Bpy2**, and **BPF** in dioxane at room temperature.

of the spectra and deactivation on the solvent at room temperature is given in Table 5.

The reason for the reduced fluorescence quantum yield is essentially not an enhanced radiationless decay rate rather than a diminished radiative rate. This becomes obvious also from the increased fluorescence lifetime in comparison with the other compounds. Also, with the larger phenanthroline derivative **Ph2**, the fluorescence rate constant differs from the value 0.60 ns^{-1} obtained from the Strickler/Berg relation. Obviously, the state populated by the absorption with the large absorptivity of 47 000 M^{-1} cm^{-1} is not the emitting or at least not the only emitting state also with **Ph2**. Possibly, there is a state inversion of closely lying nπ^* and $\pi\pi^*$ states induced by the solvent polarity. In a polar solvent the $\pi\pi^*$ state becomes the lowest one which is more efficiently emitting.

The comparison of the aza-substituted 1,4-bisphenylethinylbenzene derivatives **Py4a** and **Py3a** with the unsubstituted 1,4-bisphenylethinylbenzene as well as the comparison of the transoid bipyridines **Bpy2** and **Bpy3** with the cisoid phenanthrolines **Ph2** and **Ph3** does reveal only minor differences. This leads to the likely supposition that aza-substitution has generally a negligible effect on the spectral behavior within the class of compounds investigated. This is confirmed by the results for the biphenyl and fluorene analogues of **Bpy2** and **Ph2**. Figure 5 shows the absorption and fluorescence spectra of **BPB$_2$** and **BPF** in comparison with **Bpy2**. It turns out that the absorption spectra of **Bpy2** and **BPF** are identical in the region above 300 nm. The expected absorption of the bipyridyl subchromophore is observed at 380 nm in the spectrum of **Bpy2**. The fluorescence bands differ from each other by only a few nanometers, and their shapes are very similar. Hence it turns out that planarity of the chromophore systems is obviously the main feature determining the spectral behavior. This is demonstrated in particular with the biphenyl compound **BPB$_2$**. Similar results were obtained by Ley and Schanze with tetra-alkoxy substituted analoga to **Bpy2** and **BPB$_2$**.[22]

As known for a long time, sterical hindrance with biphenyls causes a twisted equilibrium geometry in the ground state which

TABLE 6: Results of Quantum Chemical Calculations

	transition/cm^{-1} (oscillator strength) type		
Ph1	29589 (0.06) $\pi\pi^*$	31053 (1.16) $\pi\pi^*$	33177 (0.00) nπ^*
Bpy1	30242 (2.07) $\pi\pi^*$	32762 (0.00) nπ^*	34501 (0.03) $\pi\pi^*$
Ph2	29574 (0.014) $\pi\pi^*$	30149 (2.48) $\pi\pi^*$	34146 (0.00) nπ^*
Bpy2	29096 (2.33) $\pi\pi^*$	34747 (0.00) $\pi\pi^*$	35077 (0.00) nπ^*
Bpy2a	33690 (1.78) $\pi\pi^*$	34502 (0.00) nπ^*	34503 (0.00) nπ^*
Ph3	29615 (3.21) $\pi\pi^*$	30730 (0.01) $\pi\pi^*$	30812 (0.19) $\pi\pi^*$
Bpy3	29072 (3.27) $\pi\pi^*$	33340 (0.06) $\pi\pi^*$	34742 (0.01) $\pi\pi^*$
Py3a	30434 (2.04) $\pi\pi^*$	34026 (0.00) nπ^*	34083 (0.00) $\pi\pi^*$
Bpy4	31524 (2.68) $\pi\pi^*$	35346 (0.00) $\pi\pi^*$	35664 (0.01) nπ^*
Py4a	31003 (2.04) $\pi\pi^*$	33450 (0.00) $\pi\pi^*$	33905 (0.00) $\pi\pi^*$
BPB	30391 (2.03) $\pi\pi^*$	33834 (0.01) $\pi\pi^*$	34189 (0.00) $\pi\pi^*$
BPF	29295 (2.44) $\pi\pi^*$	33250 (0.05) $\pi\pi^*$	33908 (0.03) $\pi\pi^*$
BPB$_2$	30758 (2.63) $\pi\pi^*$	34335 (0.01) $\pi\pi^*$	34593 (0.00) $\pi\pi^*$

leads to unstructured hypsochromically shifted absorption spectra. Planarization in the excited state gives rise to significantly more structured fluorescence spectra. Corresponding results were obtained for **BPB$_2$**.

Flash Photolysis. Transient absorptions with lifetimes in the range of 25−60 μs could be detected by conventional flash photolysis in deoxygenated solutions of all model compounds with low fluorescence quantum yields (**Ph1**, **Bpy1**, **Ph2**, and **Bpy2a**) in cyclohexane or toluene, which were assigned to triplet−triplet transitions because of the observed oxygen quenching and due to full reversibility after repeated flashing. However, unexpectedly, we found triplet−triplet absorption also with **Bpy2**, for instance. If we assume that the molar absorptivities for the T−T absorption maxima of **Ph2** and **Bpy2** are about the same which may not be unreasonable because of the similarity of their stationary spectral features, then the triplet quantum yield of **Ph2** in cyclohexane and toluene is only about 3−4 times larger than that of **Bpy2**. Since the fluorescence quantum yield of **Bpy2** is unity within the range of experimental error the intersystem crossing yield cannot exceed a few percent which is the error of the fluorescence quantum yield determination. Note that the detection sensitivity of the flash photolysis experiments is very high due to the intense excitation (more photons than dissolved molecules are available for excitation) and the 10 cm optical path length. Consequently, intersystem crossing is not the most efficient deactivation channel competing with fluorescence. To further confirm this conclusion we measured the T−T absorption intensity of **Ph2** as a function of temperature in the range of 20− 70 °C in order to compare it with the temperature dependence of Φ_f described above.

In contrast with the marked decrease of the fluorescence yield there was no systematic variation of the T−T absorption detectable. Thus, the thermally activated process competing with fluorescence must essentially be attributed to internal conversion.

Quantum Chemical Calculations. We have concluded from the experiments that low-lying non emitting states are the reason for the comparatively low fluorescence quantum yields of **Ph1**, **Ph2** and **Bpy2a**. To verify this conclusion and to determine the direction of the transition moments, we have performed quantum chemical calculations the results of which are presented in Table 6.

With all compounds investigated in this work are the lowest excited states predicted to have $\pi\pi^*$ configuration. In the case of the linear bipyridine derivatives, the energy gap between the lowest $\pi\pi^*$ state and the nearest nπ^* state is generally larger than the energy gaps of those states of the phenanthroline derivatives. This is due to the closer proximity of the two nitrogen lone pairs which causes a larger splitting of the two nπ^* states in comparison with the transoid bipyridine compounds. Since the singlet triplet splitting is significantly smaller with nπ^* than with $\pi\pi^*$ states, one should expect efficient isc only if the singlet triplet energy splitting exceeds the energy difference between the lowest $\pi\pi^*$ and nπ^* states. The smallest $\pi\pi^*-$nπ^* gaps are calculated for **Ph1**, **Ph2**, and **Bpy2a** which are the phosphorescent compounds. The comparatively small $\pi\pi^*-$nπ^* gap predicted for **Bpy2a** is evidently caused by a lesser conjugative stabilization of the lowest $\pi\pi^*$ state due to the meta-linkage. These are the compounds with exceptionally low fluorescence quantum yields. However, intersystem crossing is a comparatively inefficient deactivation channel also for these compounds. The calculations predict low-lying $\pi\pi^*$ states with very small oscillator strengths for these compounds which is fully in accord with the conclusions drawn from experimental findings.

If the active space for configuration interaction (C.I.) is enhanced to 1600 configurations, then the nπ^* configuration is predicted for the S_1 states of **Ph1** and **Bpy2a** with energy gaps of 200 and 400 cm^{-1}, respectively, to the nearest allowed $\pi\pi^*$ state. The forbidden $\pi\pi^*$ state becomes the S_1 state with **Ph2**. Thus, the conclusions drawn above still hold for large C.I. active space. Only one prediction is at variance with experiment: With **Py4a** the calculation predict nπ^* configuration for the S_1 state. However one should not put too much confidence on these results because with large C.I. active space the ARGUs package produces artifacts in that it mixes orthogonal orbitals.

Semiempirical calculation with twisted bipyridine geometry predict for the S_2 state of **Bpy2**, for instance, a significant admixture of nπ^*configuration. With the cisoid isomer the S_2 state is significantly closer to the S_1 state due do to the spatial proximity of the nitrogen lone pairs. The same is true for the of phenanthroline containing model compounds. Out of plain vibrational modes, particularly the torsional mode of the bipyridine rings which promote vibronic coupling between both states should be shifted to higher frequencies with phenanthroline compounds in comparison with the bipyridine analogues. Obviously, the smaller S_2-S_1 energy gap overcompensates any effects of varied vibrational frequencies active in vibronic coupling. It is impossible at our present state of knowledge to discriminate between vibronic coupling of close lying excited states interpreted as a proximity effect[23] and an activated population of the S_2 state.[24] Further investigations into the vibronic structure of the radiative transitions are in progress.

Conclusions

From a systematic variation of the chemical structure of heteroarylene and aryleneethinylenes with ethinylene, *p*-phenylene, 3- or 4-pyridyl, phenanthroline-3,8-diyl, 2,2′- bipyridine −5,5′-diyl and 2,2′- bipyridine −4,4′-diyl molecular units one can subdivide the various compounds according to their absorption properties into three classes: (i) "small compounds" consisting of one phenylethinyl unit and one 1,10-phenanthroline or 2,2′-bipyridine moiety which absorb at about 315 nm ($\epsilon \approx$ 30 000 M^{-1} cm^{-1}); (ii) compounds consisting of three 6π-(hetero)aromatic rings connected by ethinylene linkages which absorb nearly at the same wavelength, however, with enhanced absorptivity in the range of 40 000−60 000 M^{-1} cm^{-1}; (iii) compounds with the larger heteroaromatic building blocks 2,2′-bipyridine or 1,10-phenanthroline in the linear backbone which absorb at significantly longer wavelengths, the molar absorptivity being not increased. These compounds model well the absorption properties of poly-heteroarylene-ethinylenes since a further enhancement of the π system does not bring about a significant bathochromic shift.

Aza-substitution does negligibly influence the absorption properties. However, because nπ^* states come into play, isc

becomes detectable if these states are low-lying. This occurs with the small models and also with angular compounds due to diminished conjugation.

If radiationless deactivation is not negligible then internal conversion is more effective than isc. Low-lying forbidden states do contribute to ic with the very few weakly fluorescent compound of the series.

Replacing phenanthroline for 2,2′- bipyridine in the larger compounds does not alter the spectroscopic and the deactivation behavior.

Acknowledgment. Financial support by the Deutsche Forschungsgemienschaft, Sonderforschungsbereich 196, is greatly acknowledged.

References and Notes

(1) Kaes, Ch.; Katz, A.; Hosseini, M. W. *Chem. Rev.* **2000**, *100*, 3553.
(2) Balzani, V.; Juris, A.; Venturis, M. *Chem. Rev.* **1996**, *96*, 759.
(3) Grummt, U.-W.; Birckner, E.; Egbe, D. A. M.; Al-Higari, M.; Klemm, E. *J. Fluoresc.* **2001**, *11*, 41.
(4) Demas, J. N.; Crosby, G. A. *J. Phys. Chem.* **1971**, *75*, 991.
(5) Grummt, U.-W.; Feller, K.-H. *Proc. Indian Acad. Sci.* **1992**, *104*, 251.
(6) Thompson, M. A.; ARGUS, *A Quantum Chemical Electronic Structure Program*, version 1.1; 1992, available via anonymous ftp from pnlg.pnl.gov (130.20.64.11).
(7) Frisch, M. J.; Trucks, G. W.; Schlegel, H. B.; Scuseria, G. E.; Robb, M. A.; Cheeseman, J. R.; Zakrzewski, V. G.; Montgomery, J. A. Stratmann, R. E.; Burant, J. C.; Dapprich, S.; Millam, J. M.; Daniels, A. D.; Kudin, K. N.; Strain, M. C.; Farkas, O.; Tomasi, J.; Barone, V.; Cossi, M.; Cammi, R.; Mennucci, B.; Pomelli, C.; Adamo, C.; Clifford, S.; Ochterski, J.; Petersson, G. A.; Ayala, P. Y.; Cui, Q.; Morokuma, K.; Malick, D. K.; Rabuck, A. D.; Raghavachari, K.; Foresman, J. B.; Cioslowski, J.; Ortiz, J. V.; Stefanov, B. B.; Liu, G.; Liashenko, A.; Piskorz, P.; Komaromi, I.; Gomperts, R.; Martin, R. L.; Fox, D. J.; Keith, T.; Al-Laham, M. A.; Peng, C. Y.; Nanayakkara, A.; Gonzalez, C.; Challacombe, M.; Gill, P. M. W.; Johnson, B. G.; Chen, W.; Wong, M. W.; Andres, J. L.; Head-Gordon, M.; Replogle, E. S.; Pople, J. A. *Gaussian 98*, Revision A.7; Gaussian, Inc.: Pittsburgh, PA, 1998.
(8) Pautzsch, T.; Rode, C.; Klemm, E. *J. Prakt. Chem.* **1999**, *341*, 548.
(9) Tzalis, D.; Tor, Y. *Tetrahedron Lett.* **1995**, *36*, 6017.
(10) Al-Higari, M.; Birckner, E.; Heise, B.; Klemm, E. *J. Polym. Sci.: A: Polym. Chem.* **1999**, *37*, 4442.
(11) Grummt, U.-W.; Birckner, E.; Klemm, E.; Egbe, D. A. M.; Heise, B. *J. Phys. Org. Chem.* **2000**, *13*, 112.
(12) El-Ghayoury, A.;.Ziessel, R *Tetrahedron Lett.* **1997**, *38*, 2471.
(13) Egbe, D. A. M.; Klemm, E. *Des. Monomers Polymers* **2001**. In press.
(14) Nakatsuji, S.; Matsuda, K.; Uesugi, Y.; Nakashima, K.; Akiyama, S.; Fabian, W. *J. Chem. Soc., Perkin Trans.1* **1992**, 755.
(15) Perkampus, H.-H., Sandemann, I., Timmons, C. J., Eds. *DMS UV Atlas of Organic Compounds*; Butterworths: London, 1966.
(16) El-Sayed, M. A. *J. Chem. Phys.* **1963**, *38*, 2834
(17) Göller, A.; Grummt, U.-W. *Chem. Phys. Lett.* **2000**, *321*, 399.
(18) (a) Hirata, Y.; Okada, T.; Mataga, N.; Nomoto, T. *J. Phys. Chem.* **1992**, *96*, 6559. (b) Ferrante, C.; Kensy, U.; Dick, B. *J. Phys. Chem.* **1993**, *97*, 13457.
(19) Cherkasov, A. S.; Veselova, T. V.; Krasovitzkii, B. M. *Opt. Spektrosk*, **1985**, *59*, 101.
(20) Strickler, S. J.; Berg, R. A. *J. Chem. Phys.* **1962**, *37*, 814.
(21) Joshi, H. S.; Jamshidi, R.; Tor, Y. *Angew. Chem.* **1999**, *111*, 2888.
(22) Ley, K. D.; Schanze, K. S. *Coord. Chem. Rev.* **1998**, *171*, 287.
(23) Wassam, W. A.; Lim, E. C. *J. Mol. Struct.* **1978**, *47*, 129. Lim, E. C. *J. Phys. Chem.* **1986**, *90*, 6770.
(24) Seixas de Melo, J.; Becker, R. S.; Elisei, F.; Macanita, A. L. *J. Phys. Chem.* **2001**, *114*, 6063.